A Cathepsin L Isoform that Is Devoid of a Signal Peptide Localizes to the Nucleus in S Phase and Processes the CDP/Cux Transcription Factor

Brigitte Goulet,[1,7] Amos Baruch,[5,7,10]
Nam-Sung Moon,[1,8] Madeleine Poirier,[4]
Laurent L. Sansregret,[1] Ann Erickson,[6]
Matthew Bogyo,[5,9] and Alain Nepveu[1,2,3,*]
[1]Department of Biochemistry
[2]Department of Medicine
[3]Department of Oncology
[4]Department of Surgery
McGill University
687 Pine Avenue West
Montreal H3A 1A1
Canada
[5]Department of Biochemistry and Biophysics
University of California
San Francisco, California 94143
[6]Department of Biochemistry and Biophysics
University of North Carolina
Chapel Hill, North Carolina 27599

Summary

The subclass of cysteine proteases termed lysosomal cathepsins has long been thought to be primarily involved in end-stage protein breakdown within lysosomal compartments. Furthermore, few specific protein substrates for these proteases have been identified. We show here that cathepsin L functions in the regulation of cell cycle progression through proteolytic processing of the CDP/Cux transcription factor. CDP/Cux processing in situ was increased following ectopic expression of cathepsin L but was reduced in Cat L$^{-/-}$ cells. Furthermore, catalytically active cathepsin L was localized to the nucleus during the G1-S transition as detected by immunofluorescence imaging and labeling using activity-based probes. Trafficking of cathepsin L to the nucleus is accomplished through a mechanism involving translation initiation at downstream AUG sites and the synthesis of proteases that are devoid of a signal peptide. Overall, these results uncover an as yet unsuspected role for cysteine proteases in the control of cell cycle progression.

Introduction

Mammalian cysteine proteases of the papain family are targeted to the lumen of the endoplasmic reticulum via a signal peptide within their prodomain and are subsequently glycosylated, phosphorylated, and trafficked to the lysosomes (Chapman et al., 1997a). These proteases have long been thought to function exclusively in the terminal degradation of proteins in the lysosomes, but the specific phenotypes resulting from gene inactivation of different cathepsin genes have suggested that distinct cathepsins may play specific, nonredundant, physiological functions involving particular tissues or cell types (reviewed in Reinheckel et al., 2001; Turk et al., 2000). Moreover, a number of observations support the notion that cysteine proteases may also be involved in the regulatory processing of distinct protein substrates. For example, cathepsin B was recently shown to mediate protection from autolysis at the cell surface of cytotoxic T cells and natural killer cells, and cathepsin L has been found to catalyze prohormone processing in secretory vesicles of neuroendocrine cells (Balaji et al., 2002; Yasothornsrikul et al., 2003). The intriguing possibility that a cathepsin could be present in the nucleus was suggested from the findings that a nuclear serpin, MENT (myeloid and erythroid nuclear termination stage-specific protein), can efficiently inhibit a nuclear papain-like cysteine protease and cause a block in cellular proliferation (Irving et al., 2002). However, there is at present no direct evidence for the presence of a cathepsin in the nucleus.

The CDP/Cux/Cut transcription factors are a family of homeodomain proteins that are conserved among metazoans (reviewed in Nepveu, 2001). Genetic analysis in *Drosophila melanogaster* indicated that *cut* mediates phenotypic effects in a large number of tissues (Bodmer et al., 1987; Liu et al., 1991). Inactivation of *cux-1* by gene targeting in the mouse has revealed several phenotypes, including growth retardation, delayed differentiation of lung epithelia, altered hair follicle morphogenesis, male infertility, and a deficit in T and B cells (Ellis et al., 2001; Luong et al., 2002; Sinclair et al., 2001). In contrast to the small size of *cux-1* knockout mice, transgenic mice expressing *cux-1* displayed multiorgan hyperplasia and organomegaly (Ledford et al., 2002). Thus, from genetic studies both in *Drosophila* and the mouse, it is clear that the CDP/Cux/Cut gene plays an important role in tissue homeostasis in several organs.

A role for CDP/Cux in cell cycle progression, in particular at the G1/S transition, was inferred from a number of evidence. In particular, CDP/Cux binding to DNA increases at the G1/S transition (Coqueret et al., 1998; Holthuis et al., 1990; van Wijnen et al., 1996). This increase in DNA binding involves two regulatory events: dephosphorylation of the Cut homeodomain by the Cdc25A phosphatase and a specific proteolytic cleavage (Coqueret et al., 1998; Moon et al., 2001). As cells progress into S phase, a fraction of CDP/Cux p200 molecules is proteolytically processed into N-terminally truncated proteins of 110 kDa. While CDP/Cux p200 only transiently binds to DNA and carries the CCAAT-displacement activity, p110 makes a stable interaction with DNA (Moon et al., 2000, 2001). Importantly, p110 but not p200 can stimulate expression of the endogenous DNA pol α gene (Truscott et al., 2003). Thus, cell cycle-dependent processing of CDP/Cux serves to generate a p110 isoform with distinct DNA binding and transcriptional properties. However, the specific mechanisms

*Correspondence: alain.nepveu@mcgill.ca
[7]These authors contributed equally to this work.
[8]Present address: Massachusetts General Hospital, Cancer Center, 13th Street, Charlestown, Massachusetts 02129.
[9]Present address: Department of Pathology, Stanford Medical School, 300 Pasteur Drive, Stanford, California 94305.
[10]Present address: Celera Genomics, 180 Kimball Way, South San Francisco, California 94080.

and enzymes involved in proteolytic processing of CDP/Cux within the nucleus have remained largely unknown.

In the present study, we have used a number of strategies to identify the protease responsible for the S phase-specific proteolytic processing of CDP/Cux. Small molecule activity-based probes (ABPs) were used to track the activation of papain family cysteine proteases during cell cycle progression. One cysteine protease, cathepsin L, localized to the nucleus at the G1/S transition and was capable of processing CDP/Cux in vitro and in vivo to produce the physiologically relevant p110 isoform. Mechanistic studies suggest that translation initiation at downstream AUG sites allows the synthesis of shorter cathepsin L isoforms that are devoid of a signal peptide and are targeted to the nucleus as cells progress into the cell cycle. These findings uncover a hitherto unsuspected function for the "lysosomal" cysteine protease cathepsin L.

Results

Protease Inhibitors Directed against Cathepsins Inhibit CDP/Cux Processing

We first tested the effect of various protease inhibitors on the expression and activity of the CDP/Cux processed isoform p110. NIH3T3 cells were transfected with a vector, Myc-CDP-HA, expressing the full-length CDP/Cux protein with Myc and HA epitope tags at its amino and carboxy-termini, respectively. Transfected cells were treated with various protease inhibitors, and nuclear extracts were analyzed by Western blot and electrophoretic mobility shift assay (EMSA), as previously described (Moon et al., 2001). Based on steady-state levels of CDP/Cux p110 (Figure 1A) and the reduction in the intensity of the retarded complex (Figure 1A), processing was inhibited by MG132 and E-64d and to a minor extent by ALLN, cathepsin inhibitor I, and chloroquine. In contrast, lactacystin, PD150606, and EGTA had no effect, suggesting that neither the proteasome nor calpain were involved. The inhibitory effect of chloroquine appears to involve a specific function outside of the endocytic compartments since other lysosomotropic agents, like bafilomycin, bacitracin, and the proton pump inhibitor concanamycin A, did not have any effect on CDP/Cux processing (Figure 1B). In support for this notion, chloroquine but neither concanamycin A nor bafilomycin were able to inhibit CDP/Cux processing in an in vitro processing assay (Figure 2D). Thus, the overall pattern of inhibition suggested that a cathepsin-like protease could be involved in the processing of CDP/Cux.

Ectopic Expression of CDP/Cux p110 Overcomes a G1-Block Imposed by a Cysteine Protease Inhibitor

Treatment of cells with a cysteine protease inhibitor was previously reported to prevent their progression into S phase (Mellgren, 1997). Since processing of CDP/Cux was shown to take place at the G1/S transition, we tested whether forced expression of the processed CDP/Cux isoform would be able to circumvent the block imposed by a cysteine protease inhibitor (Moon et al., 2001). NIH3T3 cells stably expressing a recombinant CDP/Cux p110 protein were synchronized by serum

starvation-restimulation and the timing of their entry into S phase was monitored. Cells expressing CDP/Cux p110 started to enter in S phase at 14 hr following serum addition, whereas control cells entered in S phase at 16 hr (Figures 1C and 1D). Thus, expression of CDP/Cux p110 shortens the G1 phase coming out of quiescence. Addition of the cysteine protease inhibitor E-64d delayed the entry of control cells into S phase: at 18 hr, respectively, 24.5% and 49.3% of these cells were in S phase in the presence or absence of E-64d (Figures 1C and 1E). Cells expressing CDP/Cux p110 were less affected by the presence of E-64d, as 61.9% of these cells had progressed into S phase at 18 hr (Figure 1F). These results indicate that CDP/Cux p110 can overcome, at least partially, the G1 block that is imposed by inhibition of cysteine proteases.

Cathepsin L Can Proteolytically Process CDP/Cux In Vitro

Proteolytic processing was previously mapped to the linker region in between the CR1 and CR2 domains of CDP/Cux, and a recombinant protein containing these domains fused to a consensus nuclear localization signal was shown to be processed following transfection into NIH3T3 cells (Moon et al., 2001). Purified CR1 + CR2 recombinant protein was incubated in vitro with a panel of cathepsins. Cleaved peptides were rapidly generated following incubation with recombinant cathepsin L, K, F, and V (Figure 2A). Among the ubiquitously expressed cathepsins that were able to cleave CR1 + CR2 in vitro, F and L, cathepsin L was the most efficient. We therefore verified whether CR1 + CR2 was cleaved similarly following transfection into NIH3T3 or incubation in vitro with cathepsin L. The pTriEx-2 vector (Novagen) was used to express the same CR1 + CR2 protein in bacteria and mammalian cells. As seen in Figure 2B, the CR1 + CR2 peptides generated by cathepsin L in vitro displayed similar mobility on SDS-PAGE as the primary peptides produced following transfection into Ras-3T3 cells (compare lane 1 with lanes 4–6). N-terminal sequencing of the cleaved peptides revealed that processing occurred at three positions in vitro, following residues Q^{643}, S^{747}, and S^{755} (Figure 2D). To assess whether cathepsin L could cleave CDP/Cux at neutral pH, reactions were carried at various pH using a larger CDP/Cux substrate (Figure 2C). Although cleavage was more efficient at pH 5.5, substantial cleavage was observed at pH 7.0 and 7.5. Intriguingly, in vitro processing of CDP/Cux at pH 7.0 was inhibited not only by E-64d but also by chloroquine, raising the possibility that chloroquine can directly interfere with the reaction (Figure 2D).

Steady-State Level of the CDP/Cux Processed Isoform Correlates with Cathepsin L Expression

Coexpression of cathepsin L with Myc-CDP-HA led to an increase in the steady-state level of CDP/Cux p110 both in NIH3T3 (Figure 3A, lanes 1–3) and CV-1 cells (Figure 3A, lanes 4–6). Addition of E-64d inhibited, at least partially, the production of p110 in cells (Figure 3A, lanes 6 and 7). Importantly, cotransfection with a catalytically inactive mutant of cathepsin L, Cat L^{C25S}, did not lead to an increase in CDP/Cux p110 (Figure 3A,

A

EtOH
ALLN
MG132
Lactacystin
E-64d
PD150606
EGTA
Cathepsin Inhibitor I
Chloroquine

175—

83—

← p200
← p110

Blot: HA

EMSA: CDP/Cux

B

vector
DMSO
E-64d
Chloroquine
Concanamycin A
Bafilomycin
Bacitracin

175—

83—

← p200
← p110

Blot: HA

Myc-CDP-HA

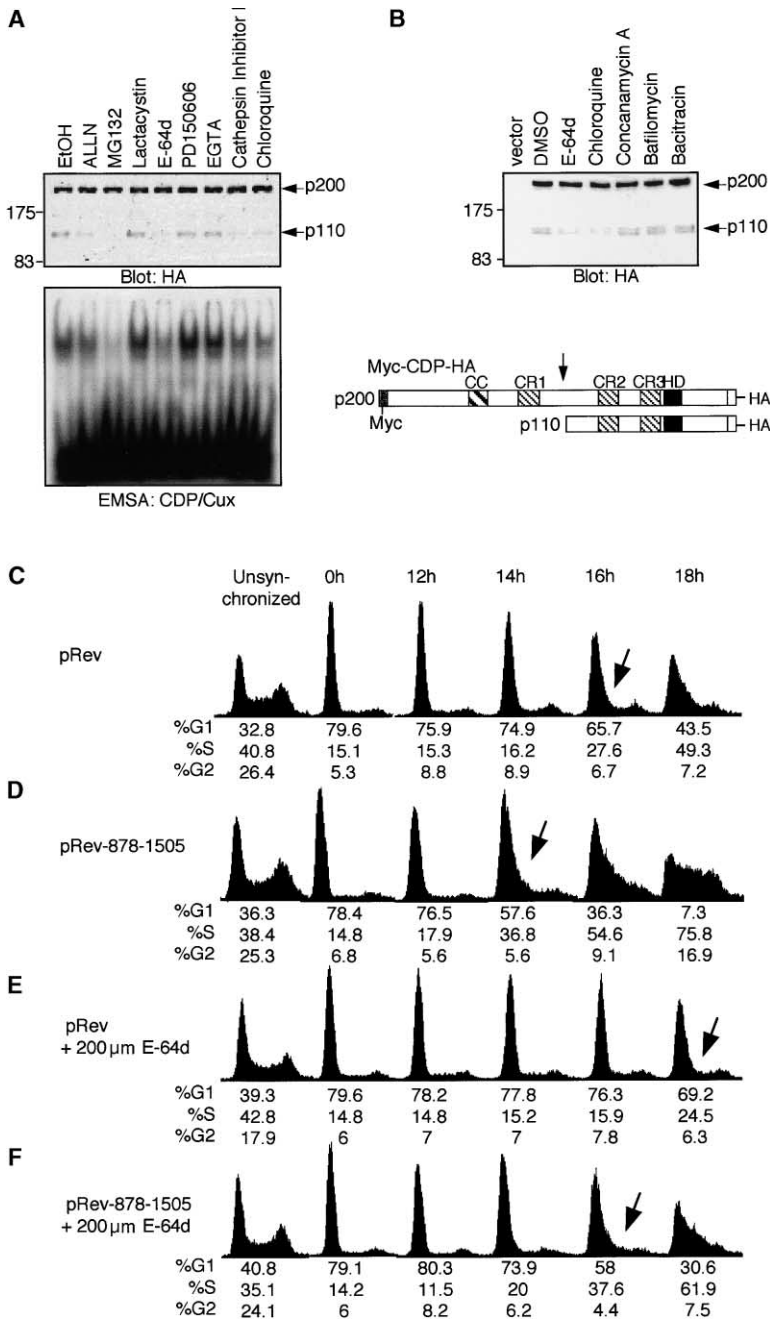p200   CC   CR1   CR2 CR3HD   ├ HA

Myc   p110   ├ HA

Figure 1. CDP/Cux Processing by a Papain Family Cysteine Protease Is Required for Its Function in Cell Cycle Regulation

(A and B) NIH3T3 cells were transfected with a vector expressing Myc-CDP-HA. The next day, cells were treated with cell-permeable protease inhibitors, and after 4 hr nuclear extracts were prepared and analyzed in Western blots with anti-HA antibodies (A, top panel) and in EMSA with the ATCGAT probe (A, bottom panel). Indicated is a schematic representation of full-length and processed CDP proteins (CC, coiled-coil; CR1, CR2, and CR3: Cut repeats 1, 2, and 3; HD, homeodomain). (C and D) Stable populations of NIH3T3 cells carrying a p110 expression vector or an empty vector were synchronized by serum starvation/restimulation. In two series of plates (E and F), the cysteine protease inhibitor E-64d was added to a final concentration of 200 μM at the same time as the fresh medium with 10% serum. At the indicated times, cells were harvested and cell cycle distribution was monitored by fluorescence-activated cell sorting (FACS) analysis after staining of the DNA with propidium iodide.

C

pRev

	Unsynchronized	0h	12h	14h	16h	18h
%G1	32.8	79.6	75.9	74.9	65.7	43.5
%S	40.8	15.1	15.3	16.2	27.6	49.3
%G2	26.4	5.3	8.8	8.9	6.7	7.2

D

pRev-878-1505

%G1	36.3	78.4	76.5	57.6	36.3	7.3
%S	38.4	14.8	17.9	36.8	54.6	75.8
%G2	25.3	6.8	5.6	5.6	9.1	16.9

E

pRev
+ 200 μm E-64d

%G1	39.3	79.6	78.2	77.8	76.3	69.2
%S	42.8	14.8	14.8	15.2	15.9	24.5
%G2	17.9	6	7	7	7.8	6.3

F

pRev-878-1505
+ 200 μm E-64d

%G1	40.8	79.1	80.3	73.9	58	30.6
%S	35.1	14.2	11.5	20	37.6	61.9
%G2	24.1	6	8.2	6.2	4.4	7.5

lane 9). Proteolytic processing of Myc-CDP-HA was also assessed in mouse embryo fibroblasts (MEF) derived from the cathepsin L knockout (Roth et al., 2000). Transfections were carried in parallel in Cat L$^{-/-}$, Cat B$^{-/-}$, and wild-type MEF cells. Proteolytic processing of Myc-CDP-HA was much less efficient in Cat L$^{-/-}$ MEF (Figure 3B). Yet, a faint band corresponding to p110 was still observed in Cat L$^{-/-}$ MEF (Figure 3B, lanes 2–4). Altogether, results from gain- and loss-of-function analysis are consistent with the notion that cathepsin L is responsible for the proteolytic processing of CDP/Cux. These results do not, however, exclude the possibility that other proteases can also proteolytically cleave CDP/Cux as demonstrated from the presence of a low amount

of CDP/Cux processed isoforms in Cat L$^{-/-}$ MEF cells (Figure 3B, lanes 2–4).

The Cathepsin L Heavy Chain Is Present at Higher Level in the Nuclear Fraction of NIH3T3 Cells that Are Enriched in S Phase

We investigated whether catalytically active cathepsin L species could be found in the nucleus. As a first approach, we used small molecule activity-based probes (ABPs) to radioactively label active papain family cathepsins directly within cells (Bogyo et al., 2000). The experiment was performed using populations of NIH3T3 cells synchronized at different points of the cell cycle (Moon et al., 2001). To help determine which of the many
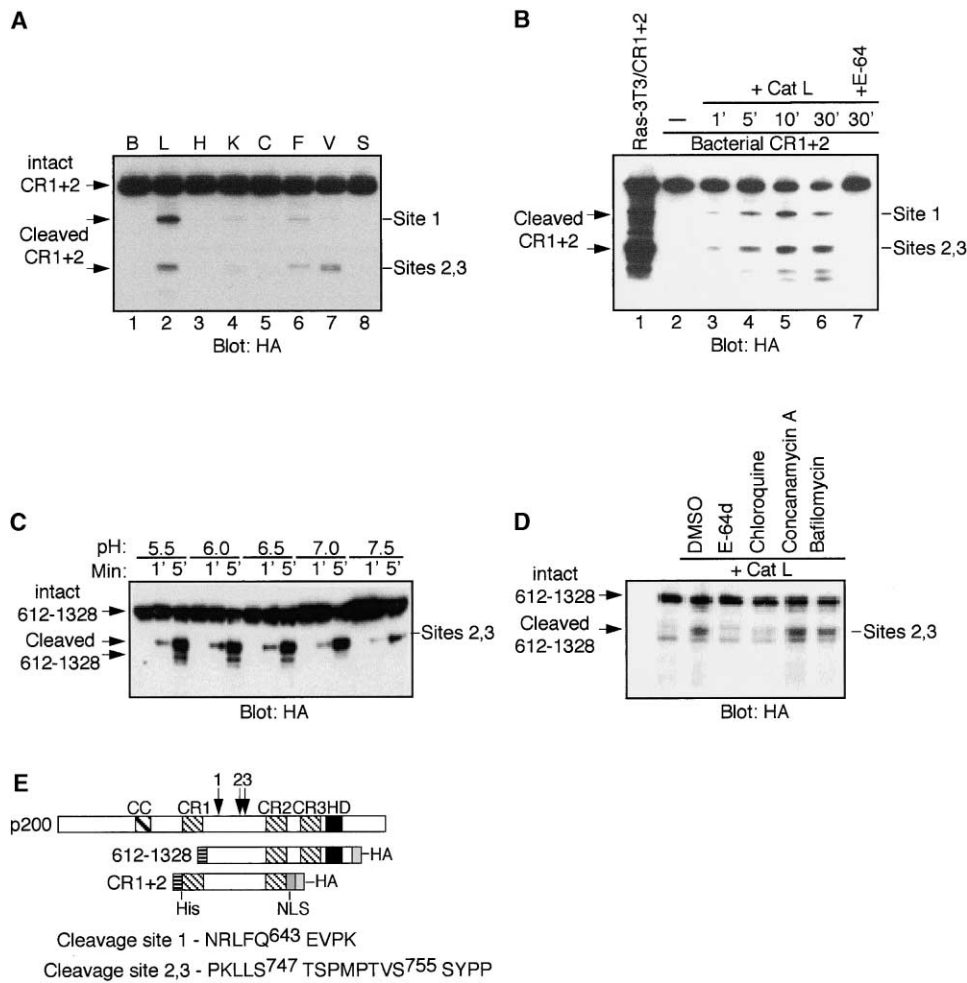
Figure 2. Cathepsin L Can Proteolytically Process CDP/Cux In Vitro

(A) CR1 + CR2-HA protein (200 ng) was incubated with various recombinant cathepsins (0.2 ng) for 10′ at RT. Samples were analyzed by Western blot using anti-HA antibody.

(B) Purified CR1 + CR2-HA protein (200 ng) was incubated with recombinant cathepsin L (0.2 ng) for 1, 5′, 10′, and 30′ at RT (lanes 2–6). A nuclear extract from Ras-3T3 cells transfected with CR1 + CR2-HA in shown for comparison (lane 1). In lane 7, 100 μM E-64 was added to the enzyme simultaneously with substrate.

(C) CDP/Cux 612-1328-HA was purified from bacteria and incubated with cathepsin L (0.2 ng) at various pH for the indicated times. Samples were analyzed by Western blot using anti-HA antibody.

(D) Purified recombinant CDP/Cux 612-1328-HA was incubated with cathepsin L (0.2 ng) at pH 7.0 for 8′ at RT in the presence of various inhibitors.

(E) Sequences of the cleavage sites identified by N-terminal sequencing of the protein fragments are indicated.

ABP-associated signals in NIH3T3 cells may correspond to cathepsin L, the experiment was performed in parallel with Cat L$^{-/-}$ MEF cells. NIH3T3 cells and Cat L$^{-/-}$ MEF were serum starved and then restimulated to enter the cell cycle. At the indicated time, cells were labeled for 1 hr with the ABP ^{125}I-JPM-OET, after which cytoplasmic and nuclear fractions were prepared and analyzed by SDS-PAGE and autoradiography (Figure 4). As expected, a number of bands were observed in the cytoplasmic fraction of both NIH3T3 and the Cat L$^{-/-}$ MEF cells (Figure 4A). Interestingly, in the nuclear fractions, two bands were present in the samples from NIH3T3 cells but were absent in the samples from Cat L$^{-/-}$ MEF cells (Figure 4B). To verify whether these bands indeed represented cathepsin L, samples from the 14 hr time points were analyzed by immunoprecipitation with anti-cathepsin L antibodies prior to analysis by SDS-PAGE. Two bands corresponding to the single and heavy chains of cathepsin L were present in the nuclear fraction of NIH3T3 cells but were not observed in the nuclear fraction of Cat L$^{-/-}$ MEF cells (Figure 4C). This experiment was repeated using wild-type and Cat L$^{-/-}$ MEFs (Figure 4D). Autoradiography with the activity-based probe (left panel) and immunoblotting with Cat L antibodies demonstrated that the single and heavy chain forms of Cat L are present in the nuclear fraction of wild-type MEFs only. Moreover, immunoblotting with anti-Lamp1 antibodies showed that the nuclear fractions
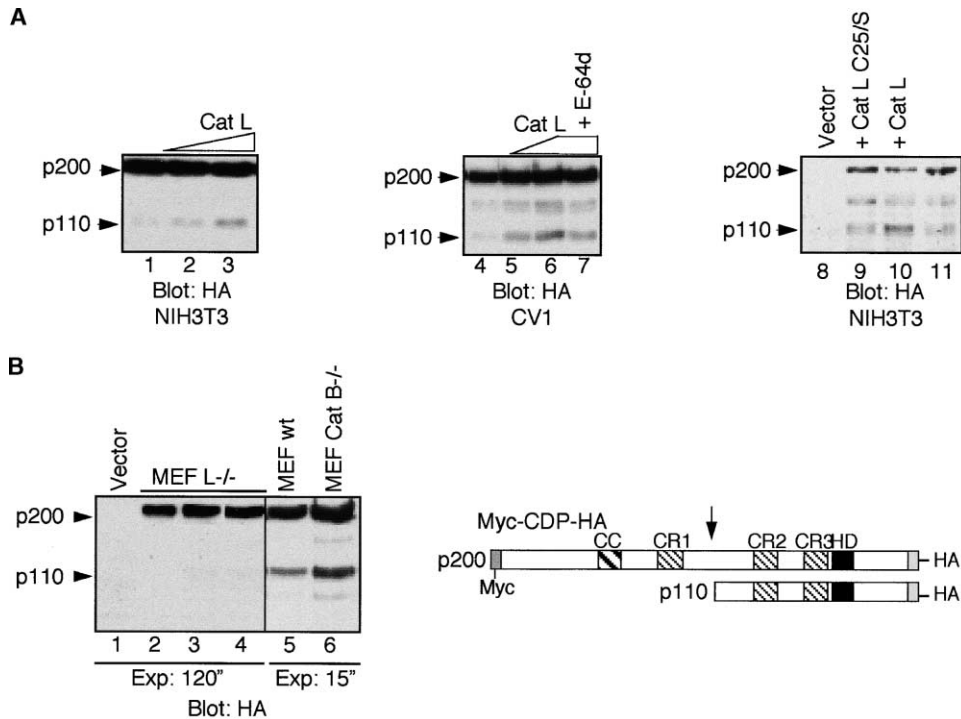
A

B

Figure 3. CDP/Cux Is Proteolytically Processed by Cathepsin L In Vivo

(A) NIH3T3 and CV1 cells were transfected with the Myc-CDP-HA vector with increasing amounts of a wild-type cathepsin L vector (lanes 2, 3, 5, 6, 7, and 10). In lane 7, cells were incubated in the presence of 20 μM of E-64d for 2 hr prior to harvesting. In lane 9, cells were cotransfected with the inactive Cat L C25/S mutant. Nuclear extracts were analyzed in Western blots with anti-HA antibodies.

(B) Wild-type MEF, MEF Cat $L^{-/-}$, and MEF cat $B^{-/-}$ cells were transfected with the Myc-CDP-HA vector. Nuclear extracts were analyzed as in (A).

were not contaminated with lysosomal proteins. Thus, active cathepsin L can be detected in the nuclear fraction of cells.

Indirect Immunofluorescence Demonstrates that the Subcellular Localization of Cathepsin L Varies during the Cell Cycle

Indirect immunofluorescence was performed on NIH3T3 cells using cathepsin L antibodies (Chapman et al., 1997b). Essentially two staining patterns were observed in continuously growing NIH3T3 cells (Figure 5B). Approximately 80% of the cells exhibited a signal consistent with lysosomal localization of cathepsin L (Erickson, 1989). In 20% of the cells, a signal was also observed over the nuclear region. The observation of different staining patterns in the same population of cells suggested that the subcellular localization of cathepsin L might vary throughout the cell cycle. NIH3T3 cells were thus synchronized by serum starvation-stimulation and monitored by indirect immunofluorescence and FACS analysis. The most frequent staining pattern for each time point is illustrated in panel 5A, while the proportion of each staining pattern is provided in panel 5B after examination of at least 200 cells at each time point (Figures 5A and 5B). We observed an increase in the proportion of cells with a nuclear staining pattern at 12, 13, and 14 hr following serum addition, when a large fraction of cells progressed beyond the G1 phase. Synchronization using an alternate method, the double thy-

midine block procedure, confirmed that a nuclear cathepsin L staining was increased in populations of cells enriched in S phase (data not shown; see also Figure 5E). Serial images at various depths demonstrated that the signal originated from within the nucleus (Figure 5C). Similar results were obtained with two other polyclonal cathepsin L antibodies directed against distinct regions of the cathepsin L protein (data not shown). Moreover, little or no signal was detected in Cat $L^{-/-}$ MEF cells (Figure 5D).

We engineered a vector, Cat L-HA, expressing cathepsin L with an HA epitope tag inserted within an external loop of the mature cathepsin L protein, at position 216 of the cathepsin L protein sequence (Coulombe et al., 1996). We confirmed that cathepsin L with this tag targets to endosomes and is secreted similarly to wt protein (A.E., unpublished observations). Moreover, the Cat L-HA protein expressed in the yeast *Pichia pastoris* was found to be enzymatically active (see below, Figure 7C). Upon transfection into NIH3T3 cells, only a fraction of cells generated a signal with the anti-HA antibody, indicating that the signal originated from transfected cells (Figure 5E). A proportion of cells expressing Cat L-HA displayed a signal in the nucleus, and this proportion increased following enrichment in S phase with double thymidine block or serum stimulation (Figure 5E). Scanning confocal microscopy demonstrated that the signal over the nuclear area was truly intranuclear (data not shown). Thus, results with three different cathepsin L antibodies and the Cat L-HA re-
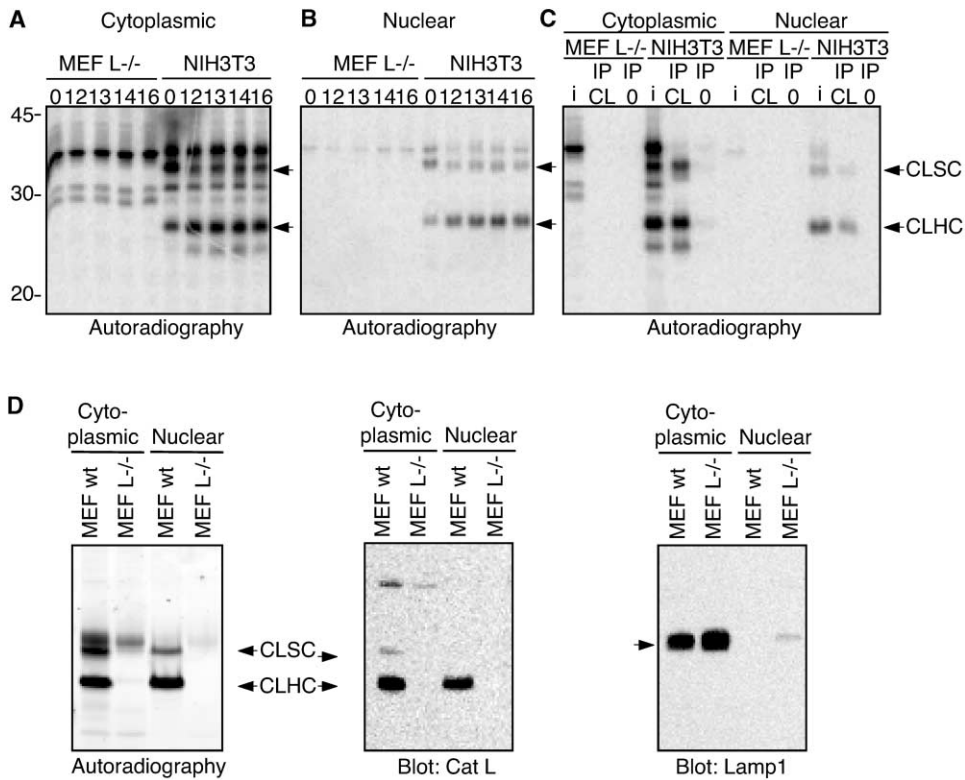
Figure 4. Cathepsin L Activity in the Nucleus Increases in a Cell Cycle-Dependent Manner

(A and B) MEF Cat L$^{-/-}$ and NIH3T3 cells were incubated for 72 hr in the absence of serum (time point 0). Serum-containing medium was added, and, at the indicated time points, cells were incubated with 10^6 counts/ml ^{125}I-JPM-OET activity-based probe for 1 hr at 37°C. Cytosolic and nuclear fractions were resolved on 14% SDS-PAGE.

(C) ^{125}I-JPM-OET-labeled nuclear and cytosolic extracts from the 14 hr time point were subjected to immunoprecipitation using cathepsin L antibodies (IP CL lanes) and control normal mouse serum (IP 0 lanes). Full-length cathepsin L single chain form (CLSC) and the C-terminally truncated heavy chain form (CLHC) are labeled with arrows at right.

(D) Intact cells were labeled with the fluorescent-conjugated DCG-04 activity-based probe. Cell lysates were separated on 12% SDS-PAGE. Gels were scanned using a Typhoon fluorescent scanner (left panel) or analyzed by immunoblotting using anti-Cat L antibodies (middle panel) or antibodies against the lysosomal marker Lamp1 (right panel).

combinant protein revealed that cathepsin L can localize to the nucleus in a cell cycle-dependent manner.

Translation Can Initiate at Internal Start Sites within the Cathepsin L mRNA

Using the cathepsin L cDNA in an in vitro transcription/translation system, we detected two bands of faster mobility that could correspond to cathepsin L proteins generated from translation initiation at sites downstream from the first AUG start codon (Figure 6A, lane 2). We performed in vitro mutagenesis to remove putative translation initiation sites from the cathepsin L cDNA. The 5′ portion of the murine cathepsin L cDNA contains 7 AUG codons, corresponding to methionine 1, 56, 58, 75, 77, 83, and 111. Replacement of the first AUG codon with UUC (M1) prevented expression of the slowest species, confirming that this band corresponds to the full-length cathepsin L (Figure 6A, lane 3). Yet, the two faster migrating species were still produced by this mutant, indicating that translation indeed could start at downstream positions. Replacement of AUG codons 56 and

58, 75 and 77 with UUC greatly reduced expression of these shorter species; however, a weak band could still be observed (Figure 6A, lane 4). Additional replacements at methionine codons 83 and 111 caused the disappearance of this band but new faster species appeared (Figure 6A, lanes 5 and 6). However, in the context of a cDNA in which the methionine codon 1 was left intact, replacement of methionine codons 56, 58, 75, 77, 83, and 111 was sufficient to eliminate expression of shorter cathepsin L species (Figure 6A, lanes 7–9). These results demonstrated that translation could start in vitro at several downstream AUG initiation sites within the cathepsin L mRNA.

Following transfection of the Cat L-HA and M1-HA plasmids into NIH3T3, we observed cathepsin L species of similar electrophoretic mobility as that seen in the in vitro system (Figure 6B, compare lanes 1 and 2 with lanes 4 and 5). We then verified whether short cathepsin L proteins are expressed from the endogenous gene. Following in vivo labeling with ^{35}S-methionine and immunoprecipitation with cathepsin L antibodies, we de-
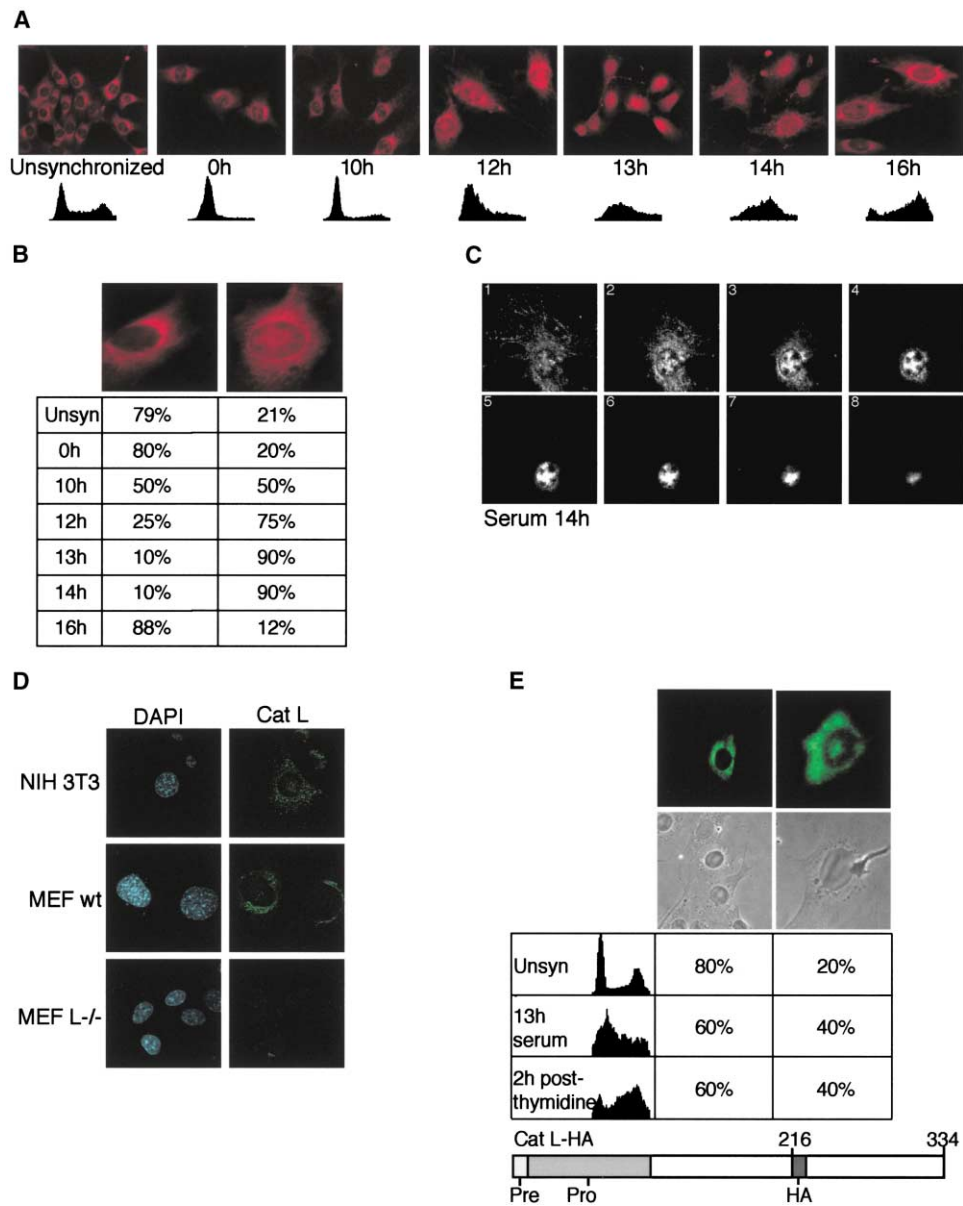
Figure 5. Evidence from Indirect Immunofluorescence that Cathepsin L Translocates to the Nucleus in NIH 3T3 Cells in a Cell Cycle-Dependent Manner

(A) NIH3T3 cells were plated on a glass cover slips and synchronized by serum starvation/stimulation. Indirect immunofluorescence was performed using a cathepsin L antibody and cell cycle distribution was monitored by FACS analysis as in Figure 1. (B) Two different patterns of staining were observed. The relative percentage of cells exhibiting each staining pattern was calculated upon examination of a minimum of 200 cells. (C) Confocal microscopy images from eight-step Z position sectional scanning of 14 hr serum-stimulated NIH3T3 cells. (D) DAPI staining and indirect immunofluorescence using a cathepsin L antibody was performed on NIH3T3, wild-type MEF, and MEF L$^{-/-}$ cells. (E) NIH3T3 cells were transfected with a vector expressing cathepsin L containing an internal HA epitope (Cat L-HA). Cells were either maintained as an unsynchronized cell population or were synchronized using either of two methods: double thymidine block followed by a 2 hr release or serum stimulation for 13 hr following a 3 day starvation period. The relative percentage of cells exhibiting each staining pattern was calculated upon examination of a minimum of 200 cells.

tected a faint band, which comigrated with a recombinant short cathepsin L species (Figure 6B, compare lane 11 with lanes 8–10). Altogether these results suggest that translation in vivo can start at downstream initiation sites within the endogenous cathepsin L mRNA, thereby allowing the synthesis of cathepsin L with distinct amino termini.

Cathepsin L Species Devoid of the Signal Peptide Are Excluded from a Membrane Fraction In Vitro and Exhibit a Distinct Subcellular Localization In Vivo
Cathepsin L proteins that start at amino acids 56, 58, 75, or 77 would not include a signal peptide and consequently should be excluded from the endoplasmic retic-
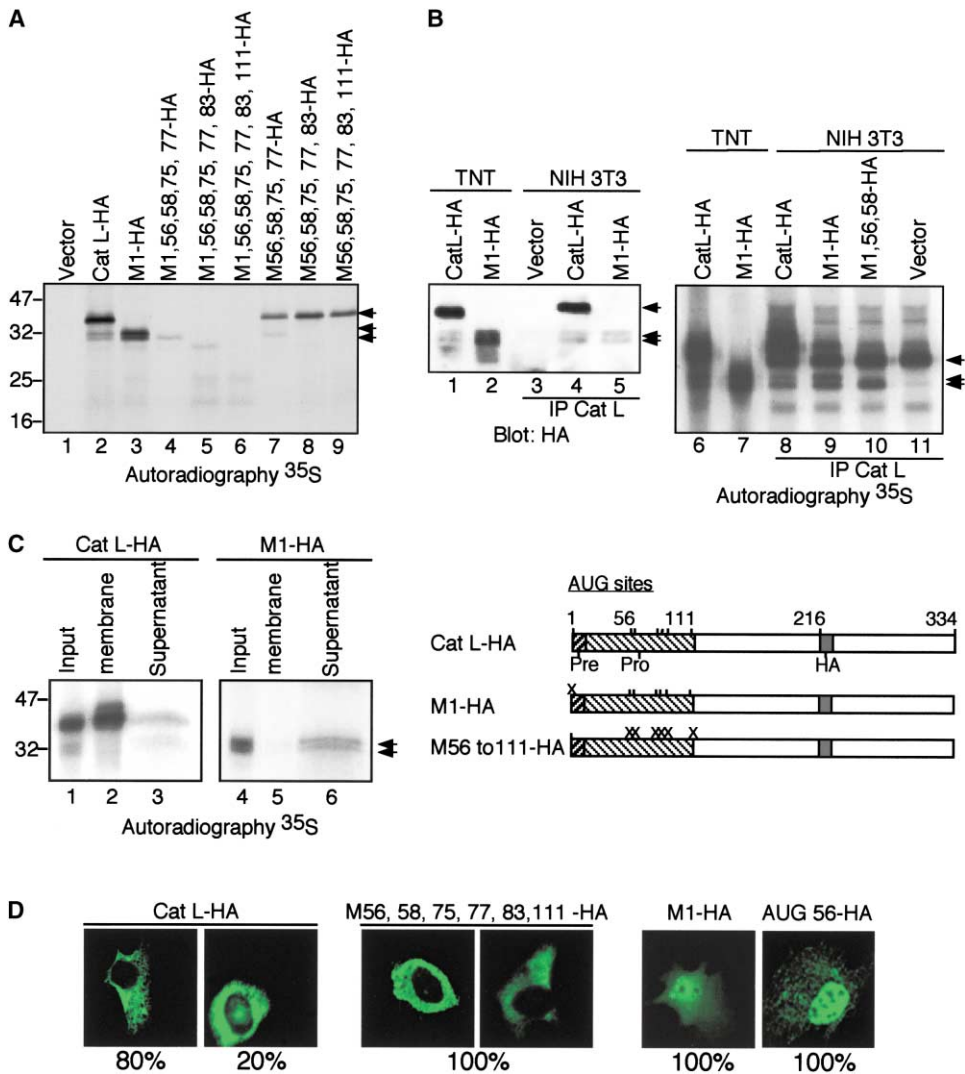
Figure 6. Translation Initiation at an Internal Start Site Allows the Expression of a Cathepsin L Isoform Devoid of the Signal Peptide

(A) Wild-type or mutated cathepsin L-HA vectors were expressed in vitro using the TNT-Promega transcription/translation system in the presence of ^{35}S-methionine and cysteine. Mutation numbers (M1, M56, etc.) refer to the methionine codons that were mutated (AUG to UUC).

(B) Wild-type and mutated Cat L-HA vectors were expressed in vitro as in (A) and in vivo in NIH3T3 cells. Cat L species were detected by autoradiography or immunoblotting with an HA antibody, as indicated. Samples from NIH3T3 cells were first immunoprecipitated with Cat L antibodies.

(C) In vitro transcription/translation with ^{35}S-methionine was performed using the Cat L-HA or M1-HA vectors with or without (input) microsomal membranes. Membranes and supernatant fractions were separated and Cat L isoforms were detected by autoradiography.

(D) Wild-type or mutated Cat L-HA vectors were introduced into NIH3T3 and indirect immunofluorescence was performed using anti-HA antibody. Representative cells are shown. In the cases where more than one staining pattern was observed, the proportion of cells exhibiting each pattern is provided.

ulum. To verify this hypothesis, in vitro translation was performed in the presence of a membrane fraction and proteins were then fractionated. As expected, the full-length cathepsin L was found mostly if not exclusively in the membrane fraction (Figure 6C, lanes 2 and 3). In contrast, the shorter cathepsin L produced by the mutant M1 were not associated with the membrane fraction and were found instead in the supernatant (Figure 6C, lanes 5 and 6). In vivo, cells transfected with the wild-type Cat L vector displayed two different staining patterns with 20% of cells showing a distinct nuclear signal

(Figure 6D). Remarkably, a strong nuclear signal was never observed in cells transfected with the mutant M56-111-HA that expresses only the full-length cathepsin L isoform (Figure 6D). In contrast, pancellular staining was observed in all cells transfected with the M1-Cat L-HA vector (Figure 6D). To confirm that nuclear staining was due to the expression of shorter cathepsin L species, we engineered a vector, AUG56, in which the cathepsin L open reading frame started at codon 56 of the wild-type cathepsin L mRNA. One hundred percent of cells transfected with this vector displayed a strong nuclear

staining pattern, thereby confirming that shorter cathepsin L species can localize to the nucleus (Figure 6D).

Cathepsin L Species Devoid of the Signal Peptide Stimulate the Processing and Transcriptional Activity of CDP/Cux

Coexpression of either wild-type or M1 Cat L-HA in NIH3T3 cells stimulated processing of the Myc-CDP-HA protein (Figure 7A, compare lanes 3–6 with lane 2). In contrast, increased processing was not observed with the M56-111-HA mutant that does not localizes to the nucleus (Figure 7A, lanes 7–9). Overall, stimulation of CDP/Cux processing correlated with the expression of shorter cathepsin L-HA isoforms as seen in Figure 7B. That the HA-tagged cathepsin L was enzymatically active was confirmed by expressing it in the yeast *Pichia pastoris* and testing it in the in vitro processing assay with CR1 + CR2 (Figure 7C, lane 3).

When wild-type cathepsin L was coexpressed with CDP/Cux p200, we observed an increase in the steady-state level of CDP/Cux p110 (Figure 7D, lane 3) and in the corresponding retarded complex as seen in electrophoretic mobility shift assay (Figure 7D, lane 7). Similarly, coexpression of AUG56-Cat L also led to an increase in CDP/Cux p110 expression and DNA binding activity (Figure 7D, lanes 12 and 17). In contrast, the M56-111 cathepsin L mutant that expresses only the full-length cathepsin L isoform was unable to stimulate CDP/Cux p110 expression and DNA binding activity (Figure 7D, lanes 13 and 18). In summary, our results demonstrate that translation initiation at downstream start sites within the cathepsin L mRNA allows the synthesis of cathepsin L isoforms that are devoid of a signal peptide (Figures 6A and 6B), do not transit through the endoplasmic reticulum (Figure 6C), can localize to the nucleus (Figure 6D), cleave the CDP/Cux transcription factor (Figure 7A), and modify its DNA binding properties (Figure 7D).

CDP/Cux Processing in a Nuclear Fraction Is Not Associated with Large-Scale Nuclear Protein Degradation

The presence of active cathepsin L in the nucleus raises an important question regarding its specificity in this compartment: does cathepsin L cleave all proteins or only a limited set? To begin to address this issue, purified cathepsin L was added to a nuclear extract at neutral pH to the point where it processed CDP/Cux, and 2D PAGE analysis was performed to assess the effect of cathepsin L on nuclear proteins in general. Western blot analysis demonstrated that CDP/Cux was efficiently processed in these conditions (Figure 7E). Comparison of nuclear proteins incubated or not with cathepsin L indicated that less than 10% of the spots disappeared or were reduced in intensity, while an equivalent number of additional spots were detected (Figure 7E). Thus, incubation of active cathepsin L with nuclear extracts at pH 7 caused the cleavage of only a small fraction of nuclear proteins. As the specificity of cathepsin L is likely to be higher in vivo in the context of a compartmentalized nucleus, these findings strongly suggest that the presence of cathepsin L in the nucleus is not associated with large-scale protein degradation.

Discussion

Expression of many cell cycle regulatory proteins is controlled in large part by their degradation (Hershko, 1997). In addition to this broad role of proteolysis in establishing distinct patterns of protein expression, our results indicate that limited proteolysis or proteolytic processing can serve in a more subtle way to modulate the biochemical properties of specific proteins during cell cycle progression. In the case of the CDP/Cux transcription factor, proteolytic processing serves to generate an isoform that is capable of making a stable interaction with DNA and engage in distinct regulatory functions (Moon et al., 2001; Truscott et al., 2003). In addition, we showed in the present study that CDP/Cux p110 was able to accelerate the G1 to S transition following exit from quiescence (Figure 1). Thus, proteolytic processing of CDP/Cux is likely to represent an important regulatory step at the onset of S phase.

The presence of active cathepsin L in the nucleus raises a number of questions regarding its processing and activity outside of the ER and lysosomal compartments. As a signal peptide is present at the N terminus of cathepsin L, the protein should be targeted to the endoplasmic reticulum during its synthesis. However, our results revealed the existence of shorter cathepsin L isoforms that are devoid of the signal peptide. The presence of faster migrating species that are generated at low efficiency from the cathepsin L mRNA in the in vitro transcription/translation system as well as in cells suggested that smaller cathepsin L isoforms may be expressed (Figure 6). Mutational analysis indicated that these smaller cathepsin L isoforms were the products of translation initiation at downstream AUG sites by a mechanism involving either leaky scanning or internal ribosome entry (Figure 6). Importantly, only shorter cathepsin L isoforms were able to translocate to the nucleus and stimulate CDP/Cux processing (Figure 6). In contrast, mutation of seven internal AUG codons lead to the expression of a full-length cathepsin L isoform that did not generate a signal in the nucleus and could not stimulate CDP/Cux processing (Figure 6). Therefore, we conclude that translation initiation at downstream AUG sites within the cathepsin L mRNA is the first requirement in the chain of events that lead to the presence of active cathepsin L in the nucleus.

A major obstacle to the correct folding and processing of shorter cathepsin L outside of the endoplasmic reticulum and lysosomes presumably would be the different redox potential and neutral pH of the cytoplasmic and nuclear milieu. While most studies on this subject have focused on activation of cathepsin L in the endosomes, proper maturation of this protease elsewhere is not impossible in light of the demonstrated autocatalytic processing of cathepsin L in vitro (Menard et al., 1998). In the latter study, autocatalytic processing required that the pH be reduced to 5.3, a situation that is unlikely to be found in the cytoplasm or the nucleus. However, we speculate that a shorter cathepsin L prodomain does not bind as tightly to the active groove, thereby allowing autocatalytic processing at higher pH. In support for this notion, a shorter form of cathepsin B that lacks the signal peptide and part of the propeptide (52 residues) was shown to fold properly and become active (Mehtani
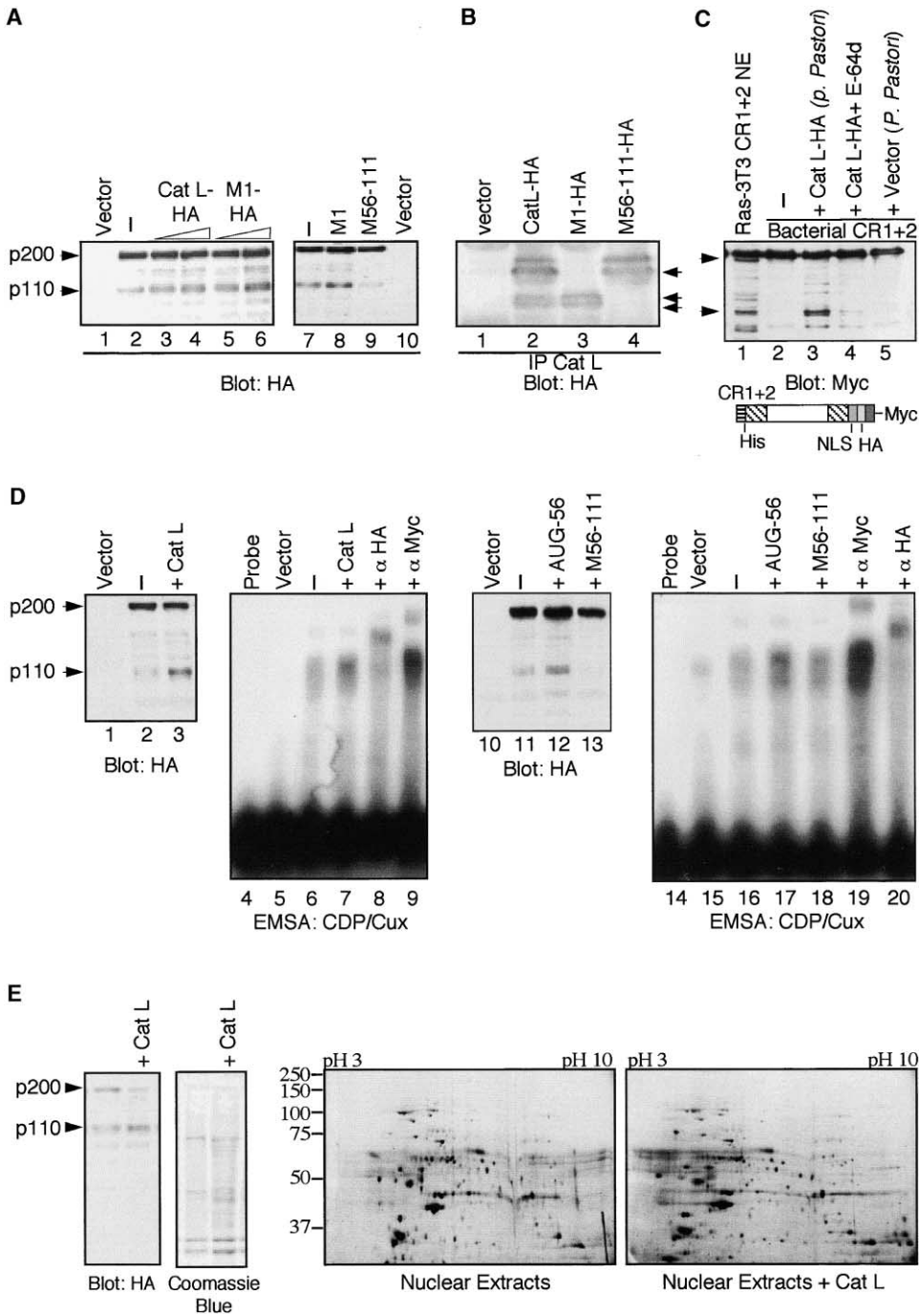
Figure 7. Short Cathepsin L Isoforms Can Process CDP/Cux and Increase Its DNA Binding Activity

(A) NIH3T3 cells were transfected with the Myc-CDP-HA vector with increasing amounts of wild-type or mutated Cat L-HA vectors. Nuclear extracts were analyzed by Western blot using anti-HA antibody.

(B) Total extracts were first submitted to immunoprecipitation with Cat L antibodies and then to immunoblotting with HA antibodies.

(C) For 10 min at 37°C, 250 ng of bacterially purified CR1 + 2-HA protein was incubated with 1 μl of media from either wild-type or Cat L-HA expressing *Pichia pastoris* in the presence or absence of E-64d. Reactions were analyzed by Western blot using anti-Myc antibodies. A nuclear extract from Ras-3T3 cells transfected with CR1 + CR2-HA in shown for comparison (lane 1).

(D) NIH3T3 cells were transfected with Myc-CDP-HA vector with or without wild-type or mutated Cat L vectors. Nuclear extracts were analyzed in Western blots with anti-HA antibodies and in EMSA as described in Figure 1.

(E) For 30′ at RT, 55 μg of nuclear extracts (NE) from Myc-CDP-HA expressing NIH3T3 cells were incubated in the presence or absence of cathepsin L (200 ng). An aliquot of 5 μg was analyzed by immunoblotting with anti-HA antibodies and Coomassie blue staining. The rest of the extract was precipitated by TCA and subjected to two-dimensional electrophoresis. Gels were stained with Sypro Ruby.

et al., 1998). As the cytosolic chaperone machinery is recruited while the nascent protein is still on the ribosome, we envisage the possibility that cytosolic chaperones somehow serve as substitutes for the proregion (Frydman, 2001). Furthermore, recent evidence suggests that a redox potential might be available in the cytosol, as members of the protein disulfide isomerase (PDI) family were found in non-ER locations, including the cytosol and the nucleus (reviewed in Turano et al., 2002). In relation to this, a number of studies have also raised the intriguing possibility that cell cycle progression from the G1 to the S phase may be associated with overall cellular (or nuclear) metabolic state/redox status (Menon et al., 2003; Zheng et al., 2003).

Can cathepsin L be a functional enzyme at neutral pH? Since optimal enzymatic activity by cathepsins is achieved at a pH 5.5, we can reasonably assume that cathepsins might only be weakly active in the nuclear milieu (Turk et al., 1997). Yet, using partially purified cathepsin L from two independent sources, rat liver and the yeast *Pichia pastoris*, we have shown that cathepsin L is able to process a CDP/Cux substrate at neutral pH, although a reduction in activity was observed at pH 7.5 relative to pH 5.5 (Figures 2C, 7C, 7E, and data not shown). We emphasize that limited cathepsin L activity in the nucleus is entirely compatible with a role in the proteolytic processing of specific nuclear proteins. In contrast, optimal activity of cathepsins in the acidic environment of the lysosome is necessary for the terminal degradation of proteins. Thus, the suboptimal pH that prevails in the nucleus should not be taken as an obstacle but rather as an important element that enables cathepsin L to play a role in the limited proteolysis of nuclear proteins. Future studies should investigate the possibility that other cysteine proteases might be present in the nucleus. In agreement with this notion, we observed a small amount of the CDP/Cux p110 isoform in Cat L$^{-/-}$ MEF cells (Figure 3B). It is possible that redundant protease activities coexist in the nucleus in a somewhat constitutive manner; alternatively, gene inactivation of cathepsin L may lead to the compensatory induction of other proteases, like cathepsin F, for example. We note that the coding sequences of cathepsin F and V contain, like cathepsin L, several AUG codons that are located downstream of the first AUG codons. Overall, our results should trigger a reevaluation of the subcellular localization of cathepsins. While it is clear that the principal activity of cathepsins takes place in the lysosomes, it is possible that alternative isoforms might avoid targeting to the ER. We further speculate that some of the phenotypes observed in the various cathepsins mutant mice might involve biochemical activities in other cellular compartments.

Experimental Procedures

Cell Culture
Cell culture, synchronizations, and FACS analysis were performed as previously described (Coqueret et al., 1998; Stein and Borun, 1972). Populations of NIH3T3 cells having stably integrated pREV/TRE-CDP/Cux 1–1505, 878–1505, or the empty pREV/TRE vector (Clontech) were generated by retroviral infection.

Preparation of Cell Extracts
Nuclear extracts were prepared according to the procedure of Lee et al. (1988) as described (Moon et al., 2001). For total extracts, cells were lysed in buffer AE (0.6% SDS, 50 mM Tris [pH 8], 100 mM NaCl, 2 mM EDTA) supplemented with a Complete™ Mini protease inhibitor cocktail tablet (Roche).

Immunoprecipitation
Polyclonal antibodies for cathepsin L (Chapman et al., 1997b) were incubated with cell extracts in AE buffer supplemented with 4% Triton X-100 and 8 mM iodoacetamide for 90 min.

Cathepsin Activity Labeling
Cathepsin activity was measured using a small activity-based probe (ABP) as previously described (Bogyo et al., 2000).

Western Blot Analysis
Protein extracts were separated by electrophoresis on 6% (CDP/Cux), 8% (CR1 + 2 and 612–1328), 12%, or 14% (cathepsin L) polyacrylamide gels. Western blot analyses with αHA (1/1000), αMyc (1/1000), and α861 (1/1000) were performed as in Moon et al. (2001) and with cathepsin L antibodies (1/20000) as in Chapman et al. (1997b).

CDP/Cux In Vitro Cleavage Assay and Cleavage Site Determination
In reaction buffer I (50 mM acetate buffer, 5 mM DTT [pH 5.5]) 200 ng of bacterially purified CR1CR2 were incubated with 0.2 ng of recombinant cathepsin L. Similar assays were performed in the presence of the recombinant cathepsins B, H, K, F, V, and S. Other buffers were used when the assay was performed at other pH: 50 mM MES at pH 5.5–6.5 and 50 mM HEPES at pH 7.0 and 7.5. To determine the sequence of cleavage sites, in vitro-generated CDP cleavage products were blotted onto a PVDF membrane and subjected to N-terminal sequencing by Edman degradation.

Two-Dimensional Electrophoresis
Immobilized pH gradient (IPG) strips (pH 3–10, 18 cm) were prepared according to the manufacturer protocol (Amersham Pharmacia Biotech). Isoelectric focusing was performed on an IPGphore system (Amersham Pharmacia Biotech). SDS-PAGE in the second dimension was performed in 8% acrylamide. Gels were stained using SYPRO Ruby according to the manufacturer protocol (Molecular Probes).

Electrophoretic Mobility Shift Assay
EMSA performed using 1 μg of nuclear extracts from transfected NIH3T3 as described (Moon et al., 2001).

Plasmid Construction
Plasmids, maps, and sequences will be provided upon request. CDP constructs Myc-CDP-HA, 878–1505, and 612–1328 have been described (Hebert et al., 2003; Moon et al., 2001). pTriEx-2/His-CR1 + 2-NLS-HA (Figure 2) contains a histidine tag, CDP amino acids 527–1027, a synthetic NLS (ALKKKRKV), and an HA tag. This clone was modified for Figure 7 by insertion of a Myc tag downstream of the HA tag. The mouse Cat L cDNA was inserted into the BamH1 site of pCDNA3 (InVitrogen). Cat L mutants were generated with the following substitutions: AUG codons (Met 1, 56, 58, 75, 77, 82, 111) were mutated to UUC (Phe) and the UGC codon of Cys 25 to UCC (Ser). AUG 56-HA was generated by PCR amplification using Cat L-HA as a template and a primer containing a Kozak consensus followed by Cat L sequences starting at AUG 56.

Pichia pastoris Expression System
Cat L-HA was introduced into the pPIC9 vector and recombinant yeast were generated and selected using the manufacturer's instructions (InVitrogen). The in vitro processing assays were performed at pH 7.0.

Immunofluorescence
NIH3T3, MEF$^{+/+}$, or MEF L$^{-/-}$ cells were plated on cover slips and transfected or not with 5 μg of wild-type or mutant pCDNA3-CatL-HA. Cells were fixed with 2% paraformaldehyde and quenched in 50 mM of NH$_4$Cl. Cells were solubilized (95% PBS + 5% FBS + 0.5% Triton X-100) and incubated with αCat L (1:1000) (Chapman

et al., 1997b), Santa Cruz D20 (1/200), Santa Cruz M19 (1/200), or αHA (1:20000) for 1 hr at RT. Secondary antibody (anti-mouse alexia 488 1:1000 or anti-rabbit alexia 594) was added for 30 min. Cells were visualized using a Zeiss AxioVert 135 microscope with a 63× objective or using a Zeiss LSM 510 confocal microscope.

In Vitro Transcription/Translation
In vitro transcription/translation was performed with ^{35}S-methionine-cysteine labeling mix (Amersham) using rabbit reticulocyte lysate-TNT kit from Promega in the absence or presence of canine pancreatic stripped microsomal membranes. Membranes were isolated as described in Kim et al. (2002).

References

Balaji, K.N., Schaschke, N., Machleidt, W., Catalfamo, M., and Henkart, P.A. (2002). Surface cathepsin B protects cytotoxic lymphocytes from self-destruction after degranulation. J. Exp. Med. *196*, 493–503.

Bodmer, R., Barbel, S., Shepherd, S., Jack, J.W., Jan, L.Y., and Jan, Y.N. (1987). Transformation of sensory organs by mutations of the cut locus of *D. melanogaster*. Cell *51*, 293–307.

Bogyo, M., Verhelst, S., Bellingard-Dubouchaud, V., Toba, S., and Greenbaum, D. (2000). Selective targeting of lysosomal cysteine proteases with radiolabeled electrophilic substrate analogs. Chem. Biol. *7*, 27–38.

Chapman, H.A., Riese, R.J., and Shi, G.P. (1997a). Emerging roles for cysteine proteases in human biology. Annu. Rev. Physiol. *59*, 63–88.

Chapman, R.L., Kane, S.E., and Erickson, A.H. (1997b). Abnormal glycosylation of procathepsin L due to N-terminal point mutations correlates with failure to sort to lysosomes. J. Biol. Chem. *272*, 8808–8816.

Coqueret, O., Berube, G., and Nepveu, A. (1998). The mammalian Cut homeodomain protein functions as a cell-cycle dependent transcriptional repressor which downmodulates p21WAF1/CIP1/SDI1 in S phase. EMBO J. *17*, 4680–4694.

Coulombe, R., Grochulski, P., Sivaraman, J., Menard, R., Mort, J.S., and Cygler, M. (1996). Structure of human procathepsin L reveals the molecular basis of inhibition by the prosegment. EMBO J. *15*, 5492–5503.

Ellis, T., Gambardella, L., Horcher, M., Tschanz, S., Capol, J., Bertram, P., Jochum, W., Barrandon, Y., and Busslinger, M. (2001). The transcriptional repressor CDP (Cutl1) is essential for epithelial cell differentiation of the lung and the hair follicle. Genes Dev. *15*, 2307–2319.

Erickson, A.H. (1989). Biosynthesis of lysosomal endopeptidases. J. Cell. Biochem. *40*, 31–41.

Frydman, J. (2001). Folding of newly translated proteins in vivo: the role of molecular chaperones. Annu. Rev. Biochem. *70*, 603–647.

Hebert, S., Bérubé, G., and Nepveu, A. (2003). Development of an in vitro assay for the proteolytic processing of the CDP/Cux transcription factor. J. Biochem. Mol. Biol. *36*, 390–398.

Hershko, A. (1997). Roles of ubiquitin-mediated proteolysis in cell cycle control. Curr. Opin. Cell Biol. *9*, 788–799.

Holthuis, J., Owen, T.A., van Wijnen, A.J., Wright, K.L., Ramsey-Ewing, A., Kennedy, M.B., Carter, R., Cosenza, S.C., Soprano, K.J., Lian, J.B., et al. (1990). Tumor cells exhibit deregulation of the cell cycle histone gene promoter factor HiNF-D. Science *247*, 1454–1457.

Irving, J.A., Shushanov, S.S., Pike, R.N., Popova, E.Y., Bromme, D., Coetzer, T.H., Bottomley, S.P., Boulynko, I.A., Grigoryev, S.A., and Whisstock, J.C. (2002). Inhibitory activity of a heterochromatin-associated serpin (MENT) against papain-like cysteine proteinases affects chromatin structure and blocks cell proliferation. J. Biol. Chem. *277*, 13192–13201.

Kim, S.J., Mitra, D., Salerno, J.R., and Hegde, R.S. (2002). Signal sequences control gating of the protein translocation channel in a substrate-specific manner. Dev. Cell *2*, 207–217.

Ledford, A.W., Brantley, J.G., Kemeny, G., Foreman, T.L., Quaggin, S.E., Igarashi, P., Oberhaus, S.M., Rodova, M., Calvet, J.P., and Vanden Heuvel, G.B. (2002). Deregulated expression of the homeobox gene Cux-1 in transgenic mice results in downregulation of p27(kip1) expression during nephrogenesis, glomerular abnormalities, and multiorgan hyperplasia. Dev. Biol. *245*, 157–171.

Lee, K.A.W., Bindereif, A., and Green, M.R. (1988). A small-scale procedure for preparation of nuclear extracts that support efficient transcription and pre-mRNA splicing. Gene Anal. Tech. *5*, 22–31.

Liu, S., McLeod, E., and Jack, J. (1991). Four distinct regulatory regions of the cut locus and their effect on cell type specification in Drosophila. Genetics *127*, 151–159.

Luong, M.X., van der Meijden, C.M., Xing, D., Hesselton, R., Monuki, E.S., Jones, S.N., Lian, J.B., Stein, J.L., Stein, G.S., Neufeld, E.J., et al. (2002). Genetic ablation of the CDP/Cux protein C terminus results in hair cycle defects and reduced male fertility. Mol. Cell. Biol. *22*, 1424–1437.

Mehtani, S., Gong, Q., Panella, J., Subbiah, S., Peffley, D.M., and Frankfater, A. (1998). In vivo expression of an alternatively spliced human tumor message that encodes a truncated form of cathepsin B. Subcellular distribution of the truncated enzyme in COS cells. J. Biol. Chem. *273*, 13236–13244.

Mellgren, R.L. (1997). Evidence for participation of a calpain-like cysteine protease in cell cycle progression through late G1 phase. Biochem. Biophys. Res. Commun. *236*, 555–558.

Menard, R., Carmona, E., Takebe, S., Dufour, E., Plouffe, C., Mason, P., and Mort, J.S. (1998). Autocatalytic processing of recombinant human procathepsin L. Contribution of both intermolecular and unimolecular events in the processing of procathepsin L in vitro. J. Biol. Chem. *273*, 4478–4484.

Menon, S.G., Sarsour, E.H., Spitz, D.R., Higashikubo, R., Sturm, M., Zhang, H., and Goswami, P.C. (2003). Redox regulation of the G1 to S phase transition in the mouse embryo fibroblast cell cycle. Cancer Res. *63*, 2109–2117.

Moon, N.S., Berube, G., and Nepveu, A. (2000). CCAAT displacement activity involves Cut repeats 1 and 2, not the Cut homeodomain. J. Biol. Chem. *275*, 31325–31334.

Moon, N.S., Premdas, P., Truscott, M., Leduy, L., Berube, G., and Nepveu, A. (2001). S phase-specific proteolytic cleavage is required to activate stable DNA binding by the CDP/Cut homeodomain protein. Mol. Cell. Biol. *21*, 6332–6345.

Nepveu, A. (2001). Role of the multifunctional CDP/Cut/Cux homeodomain transcription factor in regulating differentiation, cell growth and development. Gene *270*, 1–15.

Reinheckel, T., Deussing, J., Roth, W., and Peters, C. (2001). Towards specific functions of lysosomal cysteine peptidases: phenotypes of mice deficient for cathepsin B or cathepsin L. Biol. Chem. *382*, 735–741.

Roth, W., Deussing, J., Botchkarev, V.A., Pauly-Evers, M., Saftig, P., Hafner, A., Schmidt, P., Schmahl, W., Scherer, J., Anton-Lam-

precht, I., et al. (2000). Cathepsin L deficiency as molecular defect of furless: hyperproliferation of keratinocytes and pertubation of hair follicle cycling. FASEB J. *14*, 2075–2086.

Sinclair, A.M., Lee, J.A., Goldstein, A., Xing, D., Liu, S., Ju, R., Tucker, P.W., Neufeld, E.J., and Scheuermann, R.H. (2001). Lymphoid apoptosis and myeloid hyperplasia in CCAAT displacement protein mutant mice. Blood *98*, 3658–3667.

Stein, G.S., and Borun, T.W. (1972). The synthesis of acidic chromosomal proteins during the cell cycle of HeLa S-3 cells. I. The accelerated accumulation of acidic residual nuclear protein before the initiation of DNA replication. J. Cell Biol. *52*, 292–307.

Truscott, M., Raynal, L., Premdas, P., Goulet, B., Leduy, L., Berube, G., and Nepveu, A. (2003). CDP/Cux stimulates transcription from the DNA polymerase alpha gene promoter. Mol. Cell. Biol. *23*, 3013–3028.

Turano, C., Coppari, S., Altieri, F., and Ferraro, A. (2002). Proteins of the PDI family: unpredicted non-ER locations and functions. J. Cell. Physiol. *193*, 154–163.

Turk, B., Turk, V., and Turk, D. (1997). Structural and functional aspects of papain-like cysteine proteinases and their protein inhibitors. Biol. Chem. *378*, 141–150.

Turk, B., Turk, D., and Turk, V. (2000). Lysosomal cysteine proteases: more than scavengers. Biochim. Biophys. Acta *1477*, 98–111.

van Wijnen, A.J., van Gurp, M.F., de Ridder, M.C., Tufarelli, C., Last, T.J., Birnbaum, M., Vaughan, P.S., Giordano, A., Krek, W., Neufeld, E.J., et al. (1996). CDP/cut is the DNA-binding subunit of histone gene transcription factor HiNF-D: a mechanism for gene regulation at the G1/S phase cell cycle transition point independent of transcription factor E2F. Proc. Natl. Acad. Sci. USA *93*, 11516–11521.

Yasothornsrikul, S., Greenbaum, D., Medzihradszky, K.F., Toneff, T., Bundey, R., Miller, R., Schilling, B., Petermann, I., Dehnert, J., Logvinova, A., et al. (2003). Cathepsin L in secretory vesicles functions as a prohormone-processing enzyme for production of the enkephalin peptide neurotransmitter. Proc. Natl. Acad. Sci. USA *100*, 9590–9595.

Zheng, L., Roeder, R.G., and Luo, Y. (2003). S phase activation of the histone H2B promoter by OCA-S, a coactivator complex that contains GAPDH as a key component. Cell *114*, 255–266.